Intramolecular photon emission from a single molecule in a scanning tunneling microscope

S. W. Wu, G. V. Nazin, and W. Ho*
Department of Physics and Astronomy and Department of Chemistry, University of California, Irvine, California 92697-4575, USA
(Received 4 April 2008; published 22 May 2008)

A vibrationally resolved intramolecular photon emission from a single molecule was induced by tunneling electrons in a scanning tunneling microscope (STM). The resonant excitation of the emission was observed by tuning the bias voltage between the STM tip and the sample. The emission intensity of an individual vibronic peak goes through a maximum. The intrinsic linewidth (~3.0 meV, full width at half maximum) obtained from the emission spectra and the measured quantum yield ($\leq 1.4 \times 10^{-3}$ photon per tunneling electron) reveal the effects of different processes on the intramolecular photon emission. The comparisons between STM-induced photon emission and other techniques were made.

DOI: 10.1103/PhysRevB.77.205430 PACS number(s): 68.37.Ef, 33.50.−j, 73.20.Mf, 78.60.Fi

I. INTRODUCTION

Studies on the single-molecule level can reveal properties (such as the electronic and vibrational states) that may not be possible to obtain from ensemble averaged experiments.[1,2] Molecular photon emission such as fluorescence can be greatly enhanced or suppressed by the molecular local nanoenvironment.[3] Therefore, it would be desirable to study photon emission and simultaneously characterize the molecule and its environment with ultrahigh spatial resolution.

A scanning tunneling microscope (STM) with an additional capability of collecting photons emitted from the tunneling junction offers a unique opportunity to study optical properties of nanostructures below a 1 Å resolution.[4–8] Photons emitted from the tunneling junction are induced by the highly localized tunneling electrons when a bias voltage is applied between the STM tip and the sample. This technique has been exploited to study molecular adsorbates at surfaces.[9–13] Vibrationally resolved intramolecular photon emission was only observed from molecules that were electronically decoupled from the metallic substrate by a thin insulating film or molecular spacer.[11–13] For molecules directly adsorbed on a metal surface, intramolecular radiative transitions are quenched and surface plasmon emission excited by inelastic tunneling process (IET) dominates the optical spectra.[9,10] This clearly shows the importance of the electronic decoupling introduced by the thin insulating film and molecular spacer even though its extent has not been determined. The efficiency of such electronic decoupling is among the key parameters that determine the transient residence time of tunneling electrons in the molecule, which has a direct effect on the branching ratios for a variety of radiative and nonradiative processes associated with the electron transport through the molecules. The characterization of the residence time of a tunneling electron in the molecular state is also expected to provide an insight into the likelihood of the singlet–triplet transition, which typically has a lower quantum yield than the singlet–singlet transition in a molecular fluorescence because of the longer radiative lifetime.[13]

In this paper, we investigate the intramolecular photon emission from a single magnesium porphine (MgP) molecule adsorbed on a thin insulating alumina film that has been grown on the NiAl(110) surface and focus on how the intramolecular photon emission is affected (quenched or enhanced) by other pathways of tunneling electrons such as nonradiative decay channels and surface plasmon emission in the STM junction. In addition, we analyze the relationship between the photon emission and the tunneling spectroscopy obtained from the same molecule. We find that the intramolecular photon emission can be resonantly excited by tuning the bias voltage.

II. EXPERIMENTAL DETAILS

The experiments were conducted with a homebuilt, ultrahigh vacuum (UHV), liquid helium cooled STM operated at ~10 K. The photon emission was collected with a lens mounted inside the UHV chamber. The collected light was guided to a spectrograph (Acton Research 300) and detected with a liquid nitrogen cooled charge-coupled device chip (Princeton Instruments, Spec-10:100B). The individual optical spectra for a chosen exposure time were acquired by maintaining the STM tip over a point of interest on the sample in constant current mode [Fig. 1(a)]. During the acquisition, a relatively large positive bias voltage (V_b) was applied to the sample in order to provide sufficient energy for the tunneling electrons to excite the adsorbed molecules [Fig. 1(b)]. The STM tips were made of silver and prepared by electrochemical etching, and subsequent sputtering and annealing in UHV. The tips were further conditioned to increase the photon emission intensity by applying a series of high voltage pulses between the tip and the clean NiAl(110) surface.[11] The thin insulating alumina film (~0.5 nm thick) was prepared by exposing a clean NiAl(110) surface to 110 L (1×10^{-6} Torr for 110 s) of O_2 at 770 K and annealing to 1300 K, which resulted in an oxide film coverage of approximately 50%. The magnesium porphine (MgP) [Fig. 1(c)] molecules were thermally sublimed onto the oxidized surface at ~10 K.

III. RESULTS AND DISCUSSIONS

A. Resonant excitation of intramolecular photon emission

The complex structure of the oxide layer and the possible out-of-plane distortions in the MgP molecules result in a variety of possible molecular adsorption configurations.[14,15]

 ©2008 The American Physical Society

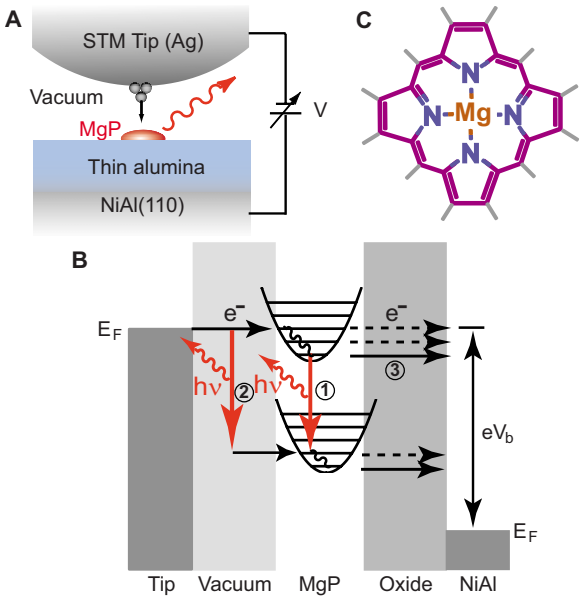

FIG. 1. (Color online) (a) Schematic sketch and (b) energy diagram of a STM junction, in which a single magnesium porphine (MgP) [its molecular structure shown in (c)] molecule is adsorbed on a thin insulating alumina film grown on a NiAl(110) surface. The STM is not only used to study this molecule via topographic imaging and tunneling spectroscopy but it is also used to probe its intramolecular radiative transition by locally exciting the molecule with tunneling electrons. Along with the intramolecular radiative transition (1), other pathways [(2) and (3)] of the tunneling electrons are marked in the diagram (details are discussed in the text).

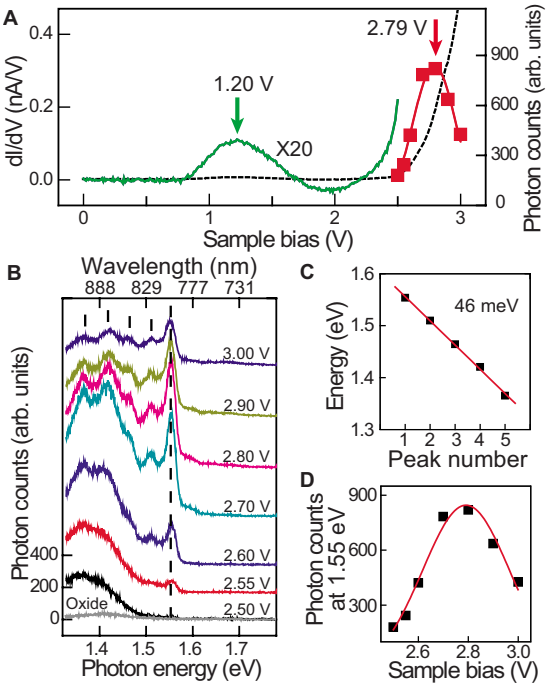

FIG. 2. (Color online) (a) dI/dV spectra measured over a single MgP molecule adsorbed on an oxidized NiAl(110) surface. The tunneling gap was set at $V_b=3.0$ V and $I=0.1$ nA. (b) A sequence of the emission spectra collected from the same molecule in (a) as a function of the bias voltage V_b marked on each spectrum. An emission spectrum (bottom) with the STM tip positioned on the bare oxide ($V_b=2.50$ V) is also shown for comparison. All spectra were acquired with $I=0.1$ nA for 300 s and are vertically offset for clarity. Individual vibronic peaks were observed with higher bias voltages and are marked in the top spectrum. The photon energy of each of the identified peaks is plotted in (c) as a function of the peak number. The slope yields a vibronic energy of 46 meV. (d) The intensity of the first vibronic peak ($h\nu=1.55$ eV) varies with the bias voltage. The profile is fitted with a Gaussian function, determining the peak at 2.79 ± 0.01 V. This plot is also shown within a larger bias range in (a).

These variations were characterized by using topographic imaging and tunneling spectroscopy with the STM.[15] The molecular states are presented as peaks in the differential conductance (dI/dV) spectra as a function of the bias voltage V_b.[16] In Fig. 2(a), the broad peak at the positive bias voltage $V_b=1.20$ V is attributed to the lowest unoccupied molecular orbital (LUMO) of the molecule.

Similar to the dI/dV spectra, the photon emission spectra that were measured from different molecules exhibited strong variations, which demonstrate the necessity of measurements at the single-molecule level. The molecular photon emission could be enhanced by tuning the bias voltage V_b. In Fig. 2(b), a sequence of the optical emission spectra for different bias voltages V_b was measured over the same molecule, as in Fig. 2(a). At $V_b=2.50$ V, the emission spectrum is dominated by a smooth broad peak. We attribute this broad peak to the local surface plasmon emission in the junction. These surface plasmons are excited through IET from the tip electronic states into the LUMO state of the molecule [pathway 2 in Fig. 1(b)].[17,18] The observed photon energy falls within the energy difference (~1.7 eV) between the tip Fermi level and the onset of the LUMO state, satisfying the energy conservation law.[19] The possibility of IET involving NiAl states underneath the oxide film is excluded because the optical spectrum, measured over the bare oxide surface, shows much weaker intensity. At higher bias voltages, a few equally-spaced narrow peaks emerge over the broad peak. These equally-spaced peaks are attributed to the individual vibronic states of the molecule, resulting from the intramolecular radiative transition from the LUMO+1 state of the molecule to the LUMO state [pathway 1 in Fig. 1(b)].[11] From the spacing of peaks in the spectra [Fig. 2(c)], the vibrational energy is determined to be 46 meV, which is assigned to the rotation and tilt motion of the pyrrole groups in MgP.[20]

As the bias voltage increases, the intensity of the intramolecular photon emission does not monotonically increase; instead, it shows a resonant peak. The intensity of the first vibronic peak at 1.55 eV is plotted as a function of the bias voltage in Fig. 2(d), which shows the peak at $V_b=2.79$ eV. This bias-dependent structure suggests that the intramolecular photon emission is strongest if the Fermi level of the tip is resonant with the molecular state on the surface such that the injection of tunneling electrons into the LUMO+1 state is most efficient. At higher bias voltages, the density of NiAl states underneath the oxide film rapidly rises,[21] which provides additional channels for the electron tunneling. This reduces the molecular excitation efficiency at a constant tunneling current. The rise of the substrate states at higher

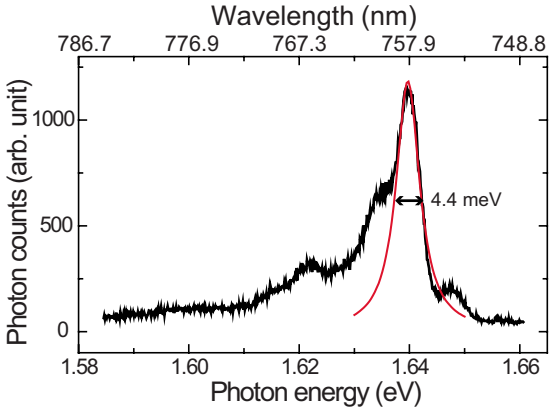

FIG. 3. (Color online) A high resolution emission spectrum from a different MgP molecule on the oxide surface. V_b=2.2 V, I =0.1 nA, and exposure time=300 s. It shows a sharp molecular emission line with a few side peaks. The dominant peak is fitted with a Lorentzian function, giving a FWHM of 4.4 meV.

voltages also obscures the higher-energy LUMO+1 molecular state in the dI/dV spectra [Fig. 2(a)] so that only the LUMO state is clearly seen at ~1.20 V. For comparison, the 1.55 eV photon emission intensity profile is plotted in the dI/dV spectra of Fig. 2(a). It can be expected that the actual position of the LUMO+1 state is close to the voltages corresponding to the emission intensity peak in Fig. 2(a). The energy difference between the LUMO+1 and the LUMO is about 1.59 eV. This value should be scaled down by a few percent if we consider the voltage drop ratio in between the vacuum gap and the oxide film, as discussed in Ref. 16. The energy difference between the LUMO+1 and the LUMO that was determined in this way is in good match with the photon energy (1.55 eV) of the first vibronic peak, which results from the radiative transition between the ground vibrational states of LUMO+1 and LUMO. This correlation between the emission and dI/dV spectra is also confirmed on those molecules with different adsorption geometries.

Resonant excitation by tuning the bias voltage leads to an enhancement of the intramolecular photon emission from individual molecules. However, other factors such as quenching and selection rules may suppress the emission while an enhancement may be possible with the plasmon excitation. The transition between LUMO+1 and LUMO in the MgP molecule is dipole allowed, as confirmed by the theoretical calculation.[22]

B. Effects of other processes on intramolecular photon emission

The decoupling of the molecules from the metal substrate by a thin alumina film enabled the observation of the intramolecular photon emission.[11] Information about the efficiency of decoupling is contained in the linewidth of the emission spectra. In Fig. 3, a high resolution emission spectrum is shown for a MgP molecule. This spectrum was taken with a 1800 grooves/mm grating, which provided a spectral resolution of 3.2 meV around 760 nm, compared to 24.3 meV with a 300 grooves/mm grating used for recording the spectra in Fig. 2(b). The high resolution spectrum shows a sharp molecular emission line with a few low energy side peaks.[23] The dominant peak is fitted with a Lorentzian function, giving a full width at half maximum (FWHM) of 4.4 meV (fitting with multiple peaks did not change the result). After deconvoluting the effect of the finite spectral resolution, the intrinsic linewidth (FWHM) of that emission line is about 3.0 meV. This number is determined by all the possible pathways of tunneling electrons in the LUMO+1 state. The total lifetime τ_{total} of tunneling electrons in the LUMO+1 state is formulated as $1/\tau_{\text{total}}=\Sigma_i 1/\tau_i$, where $1/\tau_i$ is the decay rate corresponding to the different possible decay pathways. According to the lifetime-limited linewidth transformation $[\tau_{\text{total}} \cdot \Delta E(\text{FWHM})=\hbar]$, the lifetime τ_{total} is on the order of 220 fs.

A major decay pathway of an electron in the LUMO+1 state involves tunneling from the molecule through the oxide film into the NiAl substrate [pathway 3 in Fig. 1(b)] instead of the intramolecular radiative transition (IMRT) from the LUMO+1 to the LUMO. The natural radiative lifetime τ_{IMRT} of an isolated MgP molecule is on the order of 50 ns.[22] Even if we consider the electric field enhancement as discussed later in the text, the intramolecular radiative lifetime is still much longer than the total lifetime τ_{total} of the tunneling electrons in the molecule on the surface. Other channels that can contribute to the decay of the LUMO+1 state are the intramolecular nonradiative decay and the excitation of radiative and nonradiative plasmon modes in the STM junction.

Overall, the nonradiative channels dominate over IMRT, which is suggested by the relatively low quantum yield Q of photon emission. By using a well-prepared silver tip, the quantum yield Q of radiative emission collected from a single molecule is only as high as 1.4×10^{-3} photon per tunneling electron. The quantum yield Q of intramolecular emission can be written as $Q=|\eta_E|^2\times\gamma_{\text{IMRT}}/\gamma_{\text{total}}=|\eta_E|^2\times\gamma_{\text{IMRT}}/(\gamma_{\text{nonrad}}+|\eta_E|^2\times\gamma_{\text{IMRT}})$, where γ_{IMRT} and γ_{nonrad} are the corresponding intramolecular radiative [pathway 1 in Fig. 1(b)] and total nonradiative [mainly, pathway 3 in Fig. 1(b)] decay rates, in which they are inversely proportional to their decay time ($\gamma_i=1/\tau_i$), and η_E is the electric field enhancement due to the surface plasmon resonance and the lightning rod effect localized at the tip apex. The presence of η_E in the expression for Q is based on the fact that the intensity of intramolecular photon emission from MgP is found to be proportional to the surface plasmon emission observed with the tip positioned on a clean NiAl(110) surface.[11] Given that $\tau_{\text{IMRT}}\sim50$ ns, $\tau_{\text{total}}\sim220$ fs, and $Q\sim1.4\times10^{-3}$, η_E in our experiments is on the order of 18.[24] Thus, the intramolecular radiative emission rate $|\eta_E|^2\times\gamma_{\text{IMRT}}$ is much smaller than γ_{nonrad}. The principal decay rate is governed by the nonradiative decay channels, yielding $\tau_{\text{nonrad}}\cong\tau_{\text{total}}$. The observed nonradiative lifetime τ_{nonrad} of ~220 fs has been substantiated by the theoretical calculation performed on the MgP/oxide/NiAl(110) system.[22] It is interesting to note that the nonradiative lifetime τ_{nonrad} of ~220 fs is shorter than the typical vibrational relaxation time on the order of 1~10 ps. This implies that the tunneling electron in the molecule could tunnel into the electronic states of the metal substrate even before the molecule has

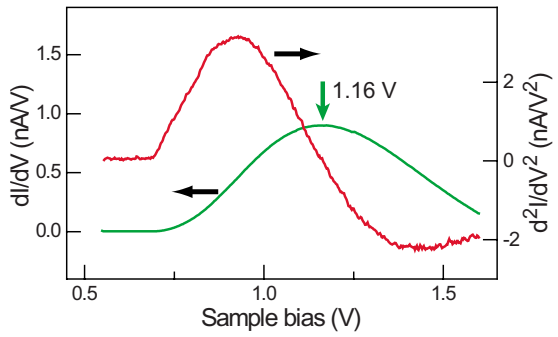

FIG. 4. (Color online) High resolution dI/dV and d^2I/dV^2 spectra measured on the same molecule as in Fig. 2. No vibronic states were resolved by tunneling spectroscopy. The tunneling gap was set at V_b=1.60 V and I=0.47 nA. The bias modulation was 10 mV (rms) at 400 Hz.

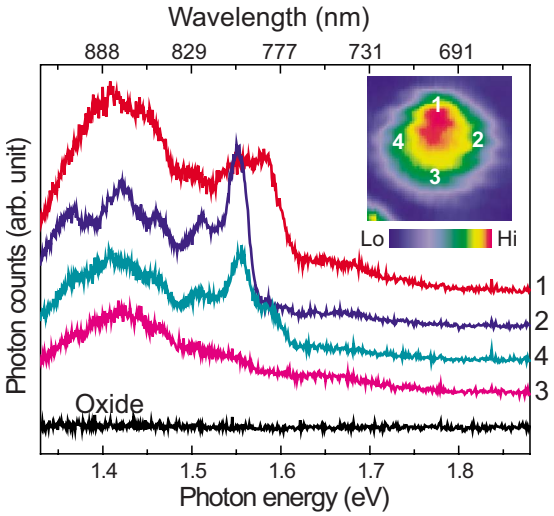

FIG. 5. (Color online) Spatial dependence of the emission spectra from the same molecule as in Fig. 2. The locations of the STM tip where each spectrum was collected are marked in the STM image of this molecule (inset). All spectra were acquired with V_b=3.0 V and I=0.1 nA for 300 s, and are vertically offset for clarity. The STM image (27 by 27 Å^2) were taken at V_b=2.25 V and I=0.1 nA. The ripples in the image are due to the coupling of the STM to the mechanical vibrations from the ground; the STM table was not floated when this image was acquired.

relaxed into the ground vibrational state of the LUMO+1 [dotted lines of pathway 3 in Fig. 1(b)]. Furthermore, this leads to a possibility of an intramolecular radiative transition from the nonrelaxed higher vibrational level in the LUMO +1 state to the LUMO state, in addition to the relaxed vibronic transition from the ground vibration level of the LUMO+1 to the LUMO state. In our experiments, the optical spectra are led by a dominant peak and followed by a few equally-spaced peaks, which resemble a Franck–Condon transition originating from the relaxed ground vibration level of the LUMO+1. However, the peaklike features on the higher-energy side of the dominant peak in Figs. 2(b) and 3 possibly result from such a nonrelaxed intramolecular radiative transition.[23] The rich dynamic processes discussed above would be anticipated in the time domain by using time-resolved techniques in future experiments.

C. Comparison to other techniques

The vibronic states of MgP can be observed not only in their photon emission spectra (as seen in Figs. 2 and 3), but also through the dI/dV tunneling spectroscopy of single molecules.[25] Figure 4 shows the dI/dV, as well as the d^2I/dV^2 spectra, measured on the LUMO state of the same molecule, as in Fig. 2. The d^2I/dV^2 spectra were recorded to increase the sensitivity to the potential presence of vibronic peaks. However, neither dI/dV nor d^2I/dV^2 shows any distinguishable vibronic structure. The vibronic states in the STM tunneling spectroscopy are not resolved because of the large number of different vibrational modes excited upon the charging of a molecule and the broadening of individual vibronic peaks.[26] In contrast, the photon emission transition occurs without a net change in the charge of the molecule, which leads to a much smaller deformation of the molecule. The vibrational excitation of the molecule occurring in the radiative transition is weaker even though both the STM tunneling spectroscopy and the photon emission spectroscopy probe the LUMO orbital of the transient molecular anion as the final state.[27] The present case demonstrates the potential and advantages of the photon emission spectroscopy, as compared to the all-electric detection in tunneling spectroscopy.

The STM-induced intramolecular photon emission differs from the photoexcited luminescence in one important aspect—the spatial resolution. Because the tunneling electrons in STM are spatially confined, the excitation occurs on the atomic scale, which could be used to resolve the internal structure of a single molecule and its chemical interaction with the neighboring environment. For example, the emission spectrum sensitively depends on the location where the STM tip is positioned inside a single molecule (Fig. 5).[11] Such ultrahigh spatial resolution, inherent in STM-induced photon emission, is a serious challenge for photoluminescence-based techniques where optical excitation is confronted with the diffraction limit. Another difference between the electric and the optical excitations lies in the different electronic transitions. In photoexcited fluorescence, the LUMO→HOMO transition of a neutral molecule is involved while the STM-induced intramolecular photon emission requires transient injection of one extra electron into a molecular state. The emission is often due to the LUMO+1→LUMO transition of a negative ion except when the bias voltage applied in the STM junction can depopulate one electron in the HOMO state.[13,16]

The use of tunneling electrons to excite the molecular adsorbates and nanostructures at surfaces and detect their photon emission in a STM could be regarded as a special cathodoluminescence technique.[28] Conventionally, cathodoluminescence is performed by using the electron beam in either a scanning electron microscope (SEM) or a scanning transmission electron microscope (STEM). The spatial resolution is limited by the electron beam diameter to a few nanometers, which is at least one order of magnitude larger than the spatial confinement of tunneling electrons in a STM.

Furthermore, the cathodoluminescence in SEM and STEM is often limited to the study of inorganic materials such as semiconductors and ceramics because the high energy electron beams (10–100 keV) could easily damage or destroy the vulnerable organic molecules. Therefore, the STM-induced light emission demonstrates superior advantages over the SEM- or STEM-based cathodoluminescence.

IV. CONCLUSIONS

In conclusion, the vibrationally resolved intramolecular photon emission is induced by tunneling electrons in a scanning tunneling microscope. The resonant excitation of the emission is observed by tuning the bias voltage between the tip and the sample. The individual vibronic peaks in the emission spectra are found to have sharp intrinsic linewidths of ~3.0 meV (FWHM) and the quantum yield of photon emission is up to 1.4×10^{-3} photon per tunneling electron. From these findings, the nonradiative molecular lifetime, as well as the electric field enhancement factor, has been estimated. A clear and detailed understanding is obtained on how the intramolecular photon emission is affected by other processes in the STM junction. This understanding is expected to impact applications where submolecular resolution and ultrasensitive chemical sensitivity are required.

ACKNOWLEDGMENTS

This material is based on work supported by the Chemical Science, Geo- and Bioscience Division, Office of Science, U.S. Department of Energy, under Grant No. DE-FG02-04ER1595.

*wilsonho@uci.edu

[1] W. E. Moerner and M. Orrit, Science **283**, 1670 (1999).
[2] W. Ho, J. Chem. Phys. **117**, 11033 (2002).
[3] P. Anger, P. Bharadwaj, and L. Novotny, Phys. Rev. Lett. **96**, 113002 (2006).
[4] J. K. Gimzewski, B. Reihl, J. H. Coombs, and R. R. Schlittler, Z. Phys. B: Condens. Matter **72**, 497 (1988).
[5] Y. Uehara, T. Fujita, and S. Ushioda, Phys. Rev. Lett. **83**, 2445 (1999).
[6] N. Nilius, N. Ernst, and H.-J. Freund, Phys. Rev. Lett. **84**, 3994 (2000).
[7] G. V. Nazin, X. H. Qiu, and W. Ho, Phys. Rev. Lett. **90**, 216110 (2003).
[8] G. Hoffmann, T. Maroutian, and R. Berndt, Phys. Rev. Lett. **93**, 076102 (2004).
[9] R. Berndt, R. Gaisch, J. K. Gimzewski, B. Reihl, R. R. Schlittler, W. D. Schneider, and M. Tschudy, Science **262**, 1425 (1993).
[10] G. Hoffmann, L. Libioulle, and R. Berndt, Phys. Rev. B **65**, 212107 (2002).
[11] X. H. Qiu, G. V. Nazin, and W. Ho, Science **299**, 542 (2003).
[12] Z.-C. Dong, X.-L. Guo, A. S. Trifonov, P. S. Dorozhkin, K. Miki, K. Kimura, S. Yokoyama, and S. Mashiko, Phys. Rev. Lett. **92**, 086801 (2004).
[13] E. Ćavar, M.-C. Blüm, M. Pivetta, F. Patthey, M. Chergui, and W.-D. Schneider, Phys. Rev. Lett. **95**, 196102 (2005).
[14] S. W. Wu, N. Ogawa, and W. Ho, Science **312**, 1362 (2006).
[15] S. W. Wu, N. Ogawa, G. V. Nazin, and W. Ho, J. Phys. Chem. C **112**, 5241 (2008).
[16] S. W. Wu, G. V. Nazin, X. Chen, X. H. Qiu, and W. Ho, Phys. Rev. Lett. **93**, 236802 (2004). A smaller scaling factor is used in the present paper due to the larger tip-molecule distance.
[17] P. Johansson, R. Monreal, and P. Apell, Phys. Rev. B **42**, 9210 (1990).
[18] B. N. J. Persson and A. Baratoff, Phys. Rev. Lett. **68**, 3224 (1992).
[19] G. Hoffmann, J. Kliewer, and R. Berndt, Phys. Rev. Lett. **87**, 176803 (2001).
[20] H.-H. Tsai and M. C. Simpson, J. Phys. Chem. A **107**, 526 (2003).
[21] N. Nilius, T. M. Wallis, M. Persson, and W. Ho, Phys. Rev. Lett. **90**, 196103 (2003).
[22] D. L. Mills, J. X. Cao, and R. Wu, Phys. Rev. B **75**, 205439 (2007).
[23] No clear assignment can be made on the side peaks although they are likely associated with low energy vibrations (~6 meV) of the molecule (Ref. 20) or phonons in the alumina. The small peak on the higher-energy side is possibly due to the nonrelaxed intramolecular radiative transition as discussed in the text or due to the lift of the LUMO orbital degeneracy when MgP is adsorbed on the surface (Ref. 14).
[24] Y. C. Martin, H. F. Hamann, and H. K. Wickramasinghe, J. Appl. Phys. **89**, 5774 (2001).
[25] X. H. Qiu, G. V. Nazin, and W. Ho, Phys. Rev. Lett. **92**, 206102 (2004).
[26] J. Repp, G. Meyer, S. Paavilainen, F. E. Olsson, and M. Persson, Phys. Rev. Lett. **95**, 225503 (2005).
[27] H. J. Lee, J. H. Lee, and W. Ho, ChemPhysChem **6**, 971 (2005).
[28] B. G. Yacobi and D. B. Holt, J. Appl. Phys. **59**, R1 (1986).